Dispersive Epidemic Waves: I. Focus Expansion within a Linear Planting

Francis J. Ferrandino

Assistant scientist, Connecticut Agricultural Experiment Station, P. O. Box 1106, New Haven, CT 06504.
Accepted for publication 2 March 1993.

ABSTRACT

Ferrandino, F. J. 1993. Dispersive epidemic waves: I. Focus expansion within a linear planting. Phytopathology 83:795-802.

The three-dimensional, turbulent dispersal of airborne spores yielded epidemiological contact distributions characterized by a length scale that continually increased with increasing downwind distance. This behavior was due to the escape of spores from the plant canopy into the faster moving air above. Such contact distributions approached an inverse power law of distance at large distances. Simulated epidemics based on this type of spore dispersal exhibited spatial disease gradients that became more shallow as the epidemic progressed. Isopathic velocities were related linearly to distance from the focus of disease, irrespective of disease severity. Thus, the leading edge of this dispersive epidemic wave propagated more quickly than did the trailing edge; as a result, the wave spread out in space with increasing time. This behavior contrasted the constant isopathic velocities characteristic of the traveling wave description predicted by spatial contact distributions of an exponential order that had a bounded length scale. A traveling wave description is appropriate if the spatial coordinate is log-transformed first.

The spread of disease from an initial point of infection depends on the dispersal of a propagule from an infected leaf to an uninfected leaf at some distance. The probability per unit area of target leaf that a spore released from a mother lesion will cause a daughter lesion at distance r is termed the contact distribution, $CD(r)$ (Table 1). The nature of the ensuing epidemic is surprisingly sensitive to the limiting behavior of this function at large distances. Mollison (30) showed that an epidemic can take the form of a traveling wave only if the tail of the contact distribution is of an exponential order such that

$$\lim_{r \to \infty} [CD(r) \exp(kr)] \to 0 \text{ for some } k > 0. \quad (1)$$

If the the condition expressed in equation 1 holds true, then the contact distribution can be characterized by the exponential length scale, $1/k_{max}$, in which k_{max} is the largest value of k for which equation 1 holds true.

To model the spread of disease from an infected plant within a row of plants, Minogue and Fry (27–29) assumed that as propagules moved in both directions away from the source, a constant fraction, p, of these propagules was deposited per plant. The deposit on the n^{th} plant, CD_n, was given by a discrete function ($CD_n = p(1 - p)^n/(2 - p)$—the double geometric distribution). Within the limit of infinitesimally small plant size, Δr, this is equivalent to a negative exponential function of distance ($r = n\Delta r$) from a foci of disease (i.e., $CD = a \exp(-a|r|)/2$, in which $a = -1\text{n}(1 - p)/\Delta r$, which in the limit gives $a = p/\Delta r$). Either of the above expressions satisfies equation 1 with an exponential length scale equal to $1/a$. The resulting epidemic could be described as a traveling wave that was approximately logistic in both time and space (14,37). The extension of the above model to two-dimensional spread of disease should account for the radial divergence of spore paths. McCartney and Bainbridge (26) suggested that a simple division by $2\pi r$ would be appropriate for this geometry (i.e., $CD_{MB} = a \exp(-a|r|)/(2\pi r)$). Such a CD satisfies equation 1 with an exponential length scale equal to $1/\alpha$. Epidemics based on this type of dispersal also can be described as traveling waves (F. J. Ferrandino, *unpublished data*).

Spore trajectories have been described by van den Bosch et al (40,41) as a two-dimensional, random walk. This assumption leads to diffusive spread away from a focus of disease. The combination of diffusive spread with diffusion coefficient ω (Table 1) and a constant relative deposition rate, δ (Table 1), leads to a modified Bessel function form for the contact distribution (i.e., $CD_V = \delta K_0[(2\delta/\omega)^{1/2}r]/(\pi\omega)$, in which K_0 is the modified Bessel function of the second type of order zero; [1]). Once again the condition expressed in equation 1 is satisfied, and the ensuing epidemic takes the form of a traveling wave (39). The added assumptions for this description to be valid are that the vector averaged wind velocity is zero and the length of time during which spores remain airborne is much larger than the time scale for changes in spore transport direction.

These models all ignore spore movement in the vertical direction (i.e., airborne spores are implicitly assumed to travel within the plant canopy), leading to the assumption that the relative rate of spore deposit per unit of time is constant. In reality, the motion of air within and above the plant canopy is three-dimensional (34,38). As spores are advected downwind, they are mixed vertically. Eventually, some spores escape from the plant canopy into the free air above, where they are not subject to deposition. The probability of an airborne spore being above the plant canopy increases with increasing downwind distance, and, therefore, the relative rate of spore deposition must decrease. The net effect of spore escape is steeper dispersal gradients near a source, due to vertical dilution of the plume of airborne spores, and a complimentary increase in deposition at larger distances, due to the eventual return of the escaped spores to the canopy. In other words, spores that escape close to the source are deposited over great distances.

Based on Sutton's theory of atmospheric dispersion (36), Gregory described the effect of vertical mixing on dispersal gradients for the spores of many plant pathogens (22,23). Chamberlain (11) and Waggoner (43) modified these results to account for depletion of airborne spores due to deposition. They obtained predicted contact distributions that approach an inverse power law of distance from the point of release at large distances and that do not fulfill the condition expressed in equation 1 (3,4,6, 7,9,15,32). The effect of such a dispersal function on focus expansion when multiple infection is not important has been studied (8). However, the impact of spore escape on more general epidemics has not been investigated.

It is the objective of this paper to use a physical model that incorporates the effects of spore escape on dispersal to 1) examine the influence of turbulent intensity and deposition rate on the validity of the traveling wave description and 2) describe the observed epidemiological behavior when traveling waves are not permissible and dispersive waves occur.

METHODS AND MATERIALS

Dispersal. I first considered a steady-state plume of spores resulting from a continuous spore release from an infinite ground-

level line source located on the y-axis ($z = 0$, $x = 0$). For the air above the plant canopy, where there is no deposition, the number of spores in a given volume of air will remain constant:

$$\partial F_x/\partial x = -(\partial F_z/\partial z) \quad (2)$$

in which F_x and F_z (Table 1) are the fluxes of spores in the x and z directions, respectively. Let $C(z,x)$ (Table 1) be the aerial concentration of spores at height z at a downwind distance, x, from the line source. In addition, let $u(z)$ (Table 1) be the horizontal wind speed and $K(z)$ (Table 1) be the coefficient of vertical turbulent mixing at height z. The horizontal flux, F_x, due to advection will be equal to the product $u(z)\ C(z,x)$, and the vertical flux, F_z, is given by $-K(z)\ \partial/\partial z[C(z,x)]$. Using these definitions, equation 2 becomes

$$u(z)\ \partial[C(z,x)]/\partial x = \partial/\partial z\{K(z)\ \partial[C(z,x)]/\partial z\}. \quad (3)$$

Assuming cylindrical symmetry for the case of two-dimensional spread from a point source and letting $C(z,r)$ (Table 1) represent the aerial concentration of spores at height z at radial distance r, equation 3 can be rewritten as

$$u(z)\ \partial[r\ C(z,r)]/\partial r = \partial/\partial z\{K(z)\ \partial[r\ C(z,r)]/\partial z\}. \quad (4)$$

Equation 4 can be solved for the case in which $u(z)$ and $K(z)$ obey the following relations (13,31,33):

$$u(z) = u_H(z/H)^{1-b},\ K(z) = K_H(z/H)^b, \quad \text{and } u_*^2 H = (1-b)u_H K_H \quad (5)$$

in which u_H is the wind speed and K_H is the coefficient of vertical turbulent mixing, both evaluated at height $z = H$, b is a dimensionless constant (~6/7) (31), and u_* (Table 1) is the friction velocity. Assuming a ground-level point release of spores from within a plant canopy of height H, the simultaneous solution of equations 4 and 5 (appendix) results in the following spatial contact distribution, including the effects of deposition:

$$CD(r) = \frac{(r/L_E^{(1-B)/2B}\ \gamma(B^{-1}, L_E/r)}{2\pi\ r\ L_D\ \Gamma(D)}$$

$$\times \exp\left\{-(L_E/L_D)\int_0^{r/LE}\left[y^{(1-B)/2B}\frac{\gamma(B^{-1}, y^{-1})}{\Gamma(D)}\right]dy\right\} \quad (6)$$

in which

$$\gamma(A,x) = \int_0^x y^{(A-1)}\ e^{-y}\ dy$$

is the incomplete gamma function of order A evaluated at x ([1], p. 260), $\Gamma(A)$ is the gamma function of A equal to $(A-1)!$ for integral A, $B = (3-2b)$, $D = (1+B)/2B = (2-b)/(3-2b)$, $L_E = u_H H^2/(B^2 K_H)$ is the downwind length scale for escape from the plant canopy (appendix), and L_D is the downwind length scale for deposit to the canopy (appendix). As is shown in the appendix, equation 6 does not fulfill the condition expressed in equation 1 and, therefore, according to Mollison (30), cannot produce traveling wave epidemics. Although equation 6 is cumber-

TABLE 1. Symbols used in this study

Symbol	Units	Description
a	m^{-1}	Mean rate of decreased deposition per unit length for the exponential contact distribution
b	ND[†]	Exponent (~6/7) in power law description of vertical turbulent diffusivity (K)
B	ND	$B = (3-2b)$
C	spores m^{-3}	Aerial spore concentration
CD	m^{-2}	Contact distribution: probability of a lesion being produced per unit area of a leaf
CD_{MB}	m^{-2}	Form of contact distribution suggested by McCartney and Bainbridge (26) given as: $CD_{MB} = a\ \exp(-ar)/(2\pi r)$
CD_V	m^{-2}	Form of contact distribution suggested by van den Bosch et al. (40) given as: $CD_V = \delta K_0[(2\delta/\omega)^{1/2} r]/(\pi w)$
D	ND	$D = (1+B)/2B = (2-b)/(3-2b)$
F_D	spores $m^{-2}\ s^{-1}$	Deposition flux of spores per unit of ground area
F_x, F_z	spores $m^{-2}\ s^{-1}$	Aerial spore flux in the x and z directions, respectively
H	m	Height of plant canopy. Use as a subscript indicates that subscripted function of height is to be evaluated at $z = H$
i	s	Infectious period
IS	m^{-2}	Infectious severity: number of spore producing lesions per unit of leaf area
K	$m^2\ s^{-1}$	Vertical turbulent diffusivity
L_D	m	Mean length of downwind travel for deposition
L_E	m	Mean length of downwind travel for escape
LS	m^{-2}	Latent severity: number of lesions that are not yet sporulating per unit of leaf area
M	ND	Multiplication factor: potential number of daughter lesions produced per mother lesion
NS	m^{-2}	Noninfectious severity: number of lesions no longer producing infectious spores per unit of leaf area
p	s	Latent period
Q	spore s^{-1}	Total outward radial flux of airborne spores
r	m	Radial distance from focus of disease
R	ND	Nondimensional distance from focus of disease: $R = r/L_E$
S	m^{-2}	Total severity: number of lesions per unit of leaf area
$SMAX$	m^{-2}	Maximum total severity: number of lesions per unit of leaf area
T	s^{-2}	Normalized time rate of release of daughter lesion producing spores per unit of time since initiation of mother lesion
u	m s^{-1}	Wind speed
u_*	m s^{-1}	Friction velocity
V	m s^{-1}	Isopathic velocity
v_d	m s^{-1}	Deposition velocity defined as F_D/C
v_g	m s^{-1}	Gravitational settling velocity of spore
z	m	Height above ground
α	s^{-1}	Logarithmic isopathic velocity
δ	s^{-1}	Mean time for spore deposition in van den Bosch model (40)
ν	ND	Measure of duration of spore release with respect to mean time between generations, τ: $\nu = i/(2\tau)$
ω	$m^{-2}\ s^{-1}$	Horizontal diffusivity in van den Bosch model (40)

[†]ND signifies that the defined quantity is dimensionless.

some to manipulate analytically, the result was numerically evaluated for use in the epidemic simulations.

The nature of an epidemic resulting from the above contact distribution (equation 6) is strongly dependent on the relative rate of spore escape to spore deposition. This is characterized by the nondimensional ratio L_E/L_D. Using $b = 6/7$ (31) in the relation between u_H and K_H given by equation 5, the definition of L_E (equation 6) gives

$$L_E = u_H H^2/B^2 K_H = (7u_H^2/81u_*^2)H. \quad (7)$$

Assuming that deposition to foliage involves gravitational sedimentation and including the effect of deposition to the ground (appendix), gives (12,18)

$$L_D = [u_H/v_g(LAI + 1)]H \quad (8)$$

in which v_g is the gravitational settling speed of spores (17) and LAI is the leaf area index of the plant canopy. For some canopies, equation 8 may have to be modified to include the contribution to deposition due to inertial impaction (25). Combining equations 7 and 8 yields

$$L_E/L_D = 7u_H v_g(LAI + 1)/81u_*^2. \quad (9)$$

Epidemiology. In addition to the contact distribution describing spore dispersal to new host tissue, an epidemiological model must account for the finite length of time during which a lesion produces spores. Let the function $T(t')$ be the rate at which new lesions produced by spores germinating at time $t - t'$ go on to release the next generation of infectious spores at time t. $T(t')$ includes the delay time needed for a germinating spore to produce sporulating lesions, as well as the time period during which lesions remain infectious. The time rate of change of lesion density S in terms of a two-dimensional analog of the logistic equation (42) is (14,15,40)

$$\frac{d[S(x,y,t)]}{dt} = \iint_{\text{all space}} CD(r') \left\{ \int_0^t T(t') \frac{d[S(x', y', t - t')]}{dt'} dt' \right\} dx'\, dy' \times [1 - S(x, y, t)/SMAX] \quad (10)$$

in which $SMAX$ is the maximum lesion density, estimated to be the total LAI of the crop divided by the mean area of a lesion; the unprimed spatial coordinates refer to the site of new infection; the primes denote the donor lesion site; and $r' = [(x - x')^2 + (y - y')^2]^{1/2}$ is the distance between donor and target lesions. The derivative of S within the time integral is the rate at which source lesions were initiated at time $t - t'$ (15). The integral over space includes the contribution of all sources to the increase in disease severity at point (x,y). Finally, the bracketed expression accounts for multiple infection.

The functional form of the time integral in equation 10, which represents the rate of inoculum production, depends on the nature of the pathogen causing the disease. In all the simulations that follow, I assume there is a latent period of duration p after infection, after which time each lesion releases M spores over an infectious period of duration i (28). For this simple case, $T(t')$ is given by the step function

$$\begin{aligned} T(t') &= 0\,;\, t' < p \\ &= M/i\,;\, p < t' < p + i \\ &= 0\,;\, p + i < t'. \end{aligned} \quad (11)$$

The effective time between generations, τ, is the first temporal moment of the function T, which for equation 11 gives $\tau = p + i/2$. Using equation 11, the solution to equation 10 can be approximated with finite difference equations (appendix). This results in a simulated epidemic in space and time. Epidemic simulations were calculated with a single-line planting of suscepts. The width and length of this strip were assumed to be 2 and 200 L_E, respectively. In these simulations, the time step, Δt, was set equal to $\tau/10$, and the line of suscepts was divided into elements of length Δr set equal to $L_E/2$.

Isopathic velocity. A useful descriptor of the rate of spread of an epidemic is the isopathic velocity, $V(S)$, defined in terms of the partial derivatives of lesion severity with respect to space and time (28):

$$V(S) = \left.\frac{dr}{dt}\right|_{\text{constant } S} = -\left.\frac{\partial S/\partial t}{\partial S/\partial r}\right|_{\substack{\text{constant r} \\ \text{constant } t}}. \quad (12)$$

It also is useful to define the logarithmic isopathic velocity, α, as

$$\alpha = V(S)/r = \{d[\ln(r)]/dt\}|_{\text{constant } S}. \quad (13)$$

RESULTS

The contact distribution given by equation 6 was evaluated numerically for values of the ratio $L_E/L_D = 4, 1, 0.25$. The results of these calculations are shown in Figure 1, in which the airborne fraction of spores is plotted versus distance. For comparison,

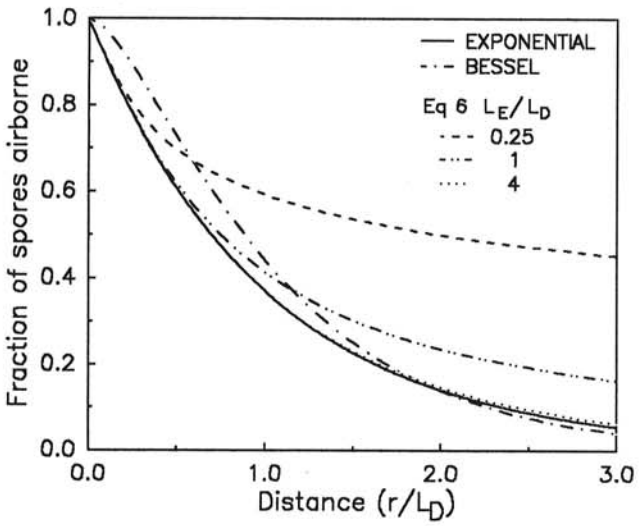

Fig. 1. The fraction of the total number of spores released that are airborne at distance r is plotted versus distance for various forms of contact distributions: $CD_{MB} = \exp(-r/L_D)/(4\pi r L_D)$: solid line; $CD_V = \delta K_0[(2\delta/\omega)^{1/2}r]/(\pi\omega)$; $(\omega/\delta)^{1/2} = L_D$: dot-dash line, and equation 6 with $L_E/L_D = 4$: dotted line; $L_E/L_D = 1$: dot-dot-dash line; and $L_E/L_D = 0.25$: dashed line.

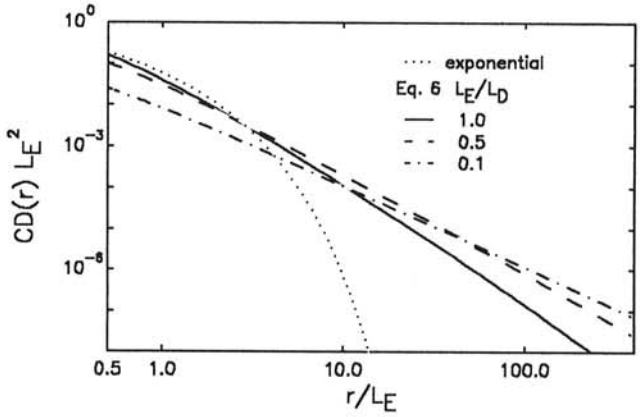

Fig. 2. Log-log plots of the contact distribution given by equation 6 versus distance for values of L_E/L_D: solid line, $L_E/L_D = 1$; dashed line, $L_E/L_D = 0.5$; dash-dot line, $L_E/L_D = 0.1$). For comparison, the modified exponential distribution suggested by McCartney and Bainbridge (26) is also shown: dotted line, $CD_{MB} = \exp(-r/L_E)/(4\pi r L_E)$.

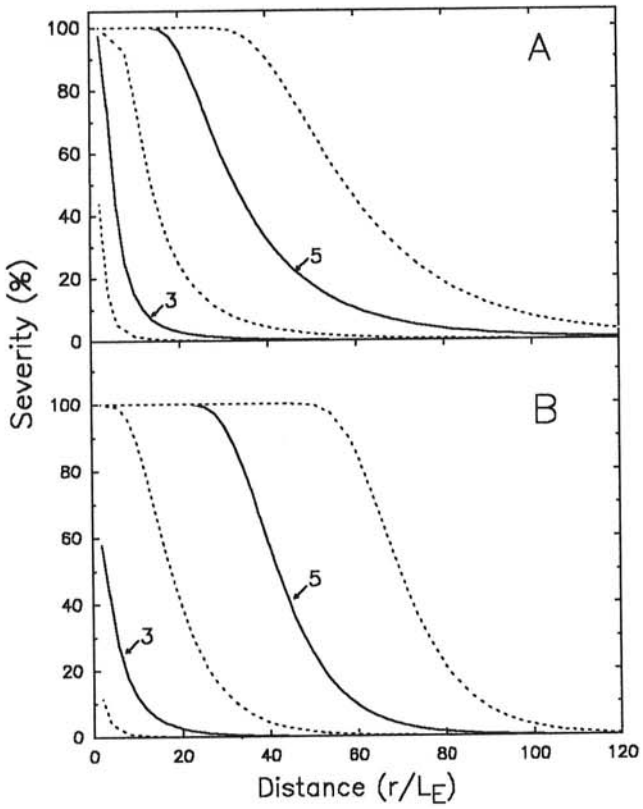

Fig. 3. Normalized lesion severity (S) versus distance, r, in simulated epidemics **A**, with CD given by equation 6 with $L_E = 0.5$ m, $L_D = 0.1$ m, and $CD_{MB} = a \exp(-ar)/(4\pi r)$ and **B**, $a = 0.5$ m^{-1}. Epidemics were seeded with $S/SMAX = 0.1$ at $t = 0$ and $r = 0$. Plots are shown for the first six generations. Generations three and five (solid lines) are labeled, and generations two, four, and six (dashed lines) are not.

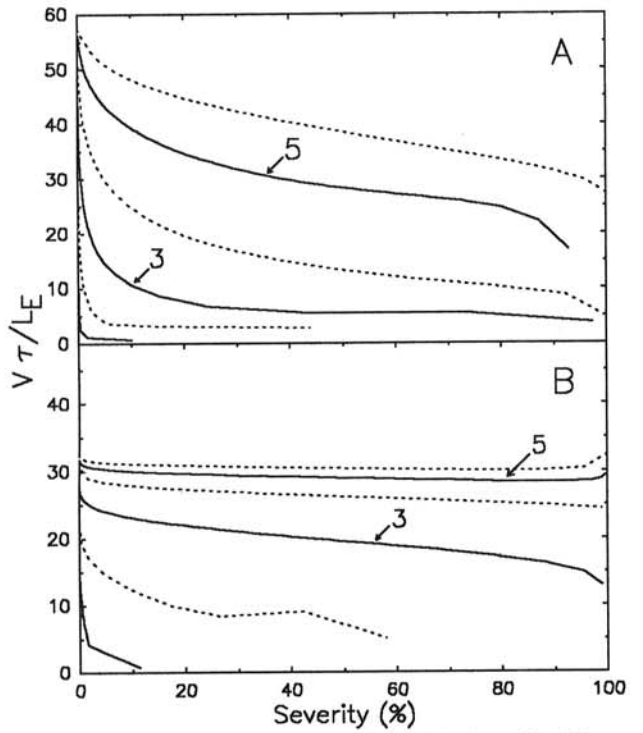

Fig. 4. Nondimensional isopathic velocity, $V\tau/L_E$ (equation 12), versus disease severity, S, for the simulations shown in Figure 3. **A** corresponds to CD given by equation 6, and **B** was generated using a modified exponential contact distribution (CD_{MB}). Plots are shown for the first six generations. Generations three and five (solid lines) are labeled, and generations two, four, and six (dashed lines) are not.

the modified exponential form suggested by McCartney and Bainbridge (CD_{MB} with $a = L_D^{-1}$; [26]) and the modified Bessel function suggested by van den Bosch et al (CD_V with $\delta/\omega = L_D^{-1}$; [40]) also are shown. When deposition dominates diffusion (i.e., $L_E/L_D > 1$), the effect of spore escape from the plant canopy is small, and the behavior of equation 6 approaches that of CD_{MB} and CD_V (Fig. 1). However, if escape is more rapid than deposition (i.e., $L_E/L_D < 1$), depletion of airborne spores is markedly reduced, and an appreciable fraction of the spores can travel a great distance from the focus.

Close to a focus, equation 6 can mimic the behavior of CD_{MB}. At large distances ($r > L_E$), however, the extended tailing behavior of equation 6 becomes important. This can be seen easily in a log-log plot of equation 6 versus distance (Fig. 2). On this type of graph, a power law produced a straight line whose slope was equal to the exponent in the power law.

Simulated epidemics resulting from CD given by equation 6 ($L_E/L_D = 1$; Fig. 3A) differed markedly from epidemics based on CD_{MB} ($a = L_E^{-1}$; Fig. 3B). Escape from the plant canopy favored the development of disease at distance, and disease gradients became shallower with each generation (Fig. 3A). Initially, the epidemic based on CD_{MB} (Fig. 3B) developed similarly. Eventually, however, the finite length scale of the dispersal function limited the downwind spread of disease. This limiting behavior was illustrated by an examination of the isopathic velocities (equation 12) for the epidemics shown in Figure 3 as a function of disease severity (Fig. 4). In the epidemic generated with equation 6 as the contact distribution, isopathic velocity continued to increase and remained dependent on disease severity (Fig. 4A). The leading edge of the disease wave always moved faster than the trailing edge. The epidemic based on CD_{MB} uniformly approached a limiting isopathic velocity (Fig. 4B).

The dispersive nature of the epidemic wave (Fig. 3) was highlighted by an examination of the spatial distribution of sporulating lesion density, IS_j^n, as a function of time. For the epidemic based on equation 6, the spatial width of the infectious region continued to spread with each generation (Fig. 5A). However, for the epidemic based on CD_{MB}, the zone of sporulation quickly reached a maximum width (Fig. 5B). This behavior was characteristic of a traveling wave.

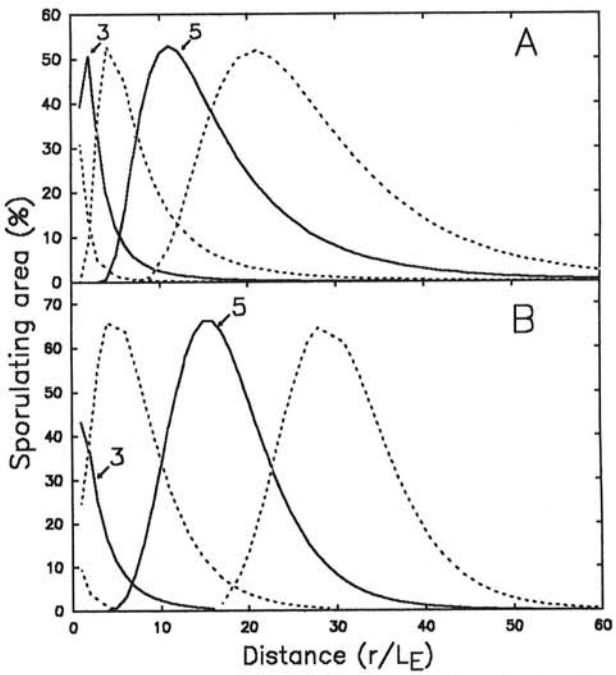

Fig. 5. Normalized infectious severity, IS, versus dimensionless distance, $r/_{LE}$, for the simulations shown in Figure 3. **A**, corresponds to equation 6. **B**, was generated using CD_{MB} (in text). Plots are shown for the first six generations. Generations three and five (solid lines) are labeled, and generations two, four, and six (dashed lines) are not.

In 96 simulated epidemics based on equation 6, isopathic velocity was a linear function of distance from the the focus of disease. The limiting slope of this linear relation was, by definition (equation 13), the logarithmic isopathic velocity α (Fig. 6; $M = 7.5$, $L_E/L_D = 0.5$, and $\nu = i/(2\tau) = 0.33$). The value of α increased with increasing multiplication factor M, increasing escape from the canopy, as characterized by the ratio L_E/L_D, and increasing infectious period, as characterized by the nondimensional ratio $\nu = i/(2\tau)$ (Fig. 7). The value of M varied from 2 to 500, L_E/L_D varied from 0.05 to 2.0 and ν ranged from 0.1 to 0.8 in the 96 simulations.

DISCUSSION

Logarithmic wave. None of the simulated epidemics based on equation 6 as the contact distribution could be described as a simple traveling wave. In every case, the calculated isopathic velocities increased linearly with increasing distance from the focus (Fig. 6) independent of the level of disease severity. Combining equations 12 and 13, I obtained

$$-\partial S/\partial t = \alpha r(\partial S/\partial r) \tag{14}$$

or

$$(\partial S/\partial t)/(\alpha r) = -(\partial S/\partial r). \tag{15}$$

For the special case α = constant (Fig. 6), because the spatial partial derivative of equation 14 must equal the temporal partial derivative of equation 15, I obtained

$$-(\partial^2 S/\partial r \partial t) = \alpha\{\partial[r(\partial S/\partial r)]/\partial r\} = (\partial^2 S/\partial t^2)/\alpha r = -\partial^2 S/\partial t \partial r. \tag{16}$$

Recalling that $d[\ln(r)]/dr = 1/r$, the inner two terms in equation 16 can be rearranged to yield

$$\partial^2 S/\partial t^2 = \alpha^2\{\partial^2 S/\partial[\ln(r)]^2\}. \tag{17}$$

Equation 17 is a form of the wave equation that admits traveling wave solutions in the log-transformed space (i.e., $S(r,t) = f[\ln(r) - \alpha t]$, for any arbitrary function f). Thus, a constant value for the logarithmic isopathic velocity, α, leads to traveling waves when disease severity is plotted against the logarithm of distance from the focus of disease. Traveling epidemic waves in the log-transformed space are consistent with the logit(S) − log(r) transformation suggested by Berger and Luke (10) and Jeger's (24) type IV epidemic. The potentially unlimited length scale of this type of epidemic is ultimately limited only by the size of the experimental plot. This rapid spread of disease may have important consequences in yield prediction models (15,16).

The measurements of potato late blight severity as presented by Minogue and Fry (29) show steep spatial disease gradients early in the epidemic that become shallower as the epidemic progresses. This is consistent with Waggoner's (43) observation that the length scale for the decrease in late blight severity about a point source grew from 0.5 m (roughly the height of a plant) for the primary disease gradients to 9 m (the size of the plots) within 24 days. An epidemic model based on the escape of spores from the plant canopy can describe this type of behavior when the finite size of the experimental plot is included. ($M = 100$, $S_0 = 0.1$, $L_E = 0.5$ m, $L_E/L_D = 0.1$, $\nu = 0.3$; Fig. 8). In examining the spread of late leaf spot in peanut, Alderman et al (2) reported an isopathic velocity of 0.09 m d^{-1} during the initial stages of the epidemic (11–22 August). During this period, disease was basically confined to within 1.5 m of the focus. An examination of Alderman et al's disease-incidence data indicates that spatial disease gradients also became less steep as the epidemic progressed (22 August through 10 September). Direct application of equation 12 to this data ([2]; Fig. 1) resulted in estimated isopathic velocities of 0.4, 0.8, and 2.9 m d^{-1} at distances of 2, 4, and 6 m from the focus of disease, respectively. After two generations of the pathogen (τ = 20d; [2]), disease incidence became fairly homogenous over the 20- × 20-m area within which disease was measured. All of the above observations are consistent with the aforemen-

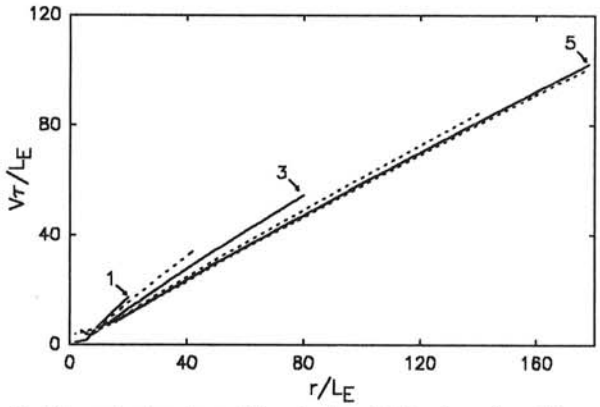

Fig. 6. Dimensionless isopathic velocity, $V\tau/L_E$ (equation 12), versus dimensionless distance from focus, r/L_E, for an epidemic simulation based on equation 6 ($L_D = L_E/2$, $M = 7.5$, $\nu = 0.33$). Plots are shown for the first six generations. Generations one, three, and five (solid lines) are labeled, and generations two, four, and six (dashed lines) are not.

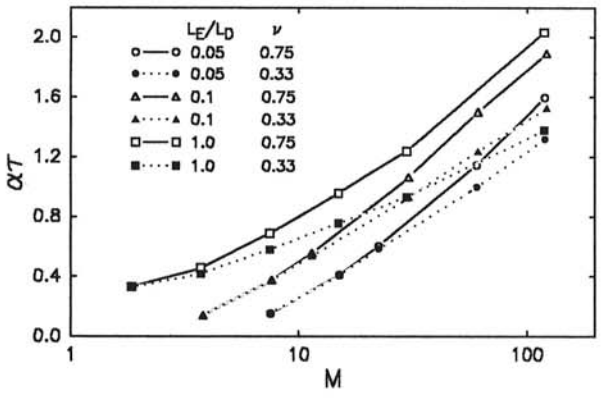

Fig. 7. The nondimensional logarithmic isopathic velocity, equation 13, versus the logarithm of the epidemic multiplication factor, M, for values of $L_E/L_D = 0.05$ (circles), 0.1 (triangles), and 1.0 (squares) and for values of $\nu = i/(2\tau) = 0.75$ (solid line-open symbols) and 0.33 (dotted line-filled symbols).

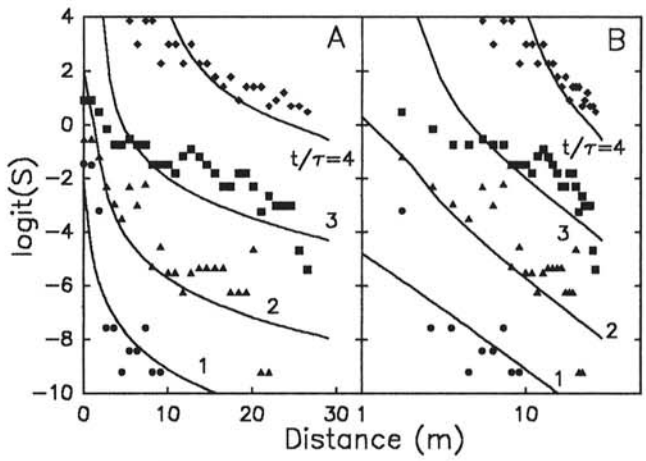

Fig. 8. A, Logit disease severity versus distance r and **B,** the natural logarithm of distance (ln(r)) for late blight on Katahdin potatoes as presented by Minogue and Fry ([29]; Fig. 2). Data from four dates are shown: 3 August (circles), 6 August (triangles), 9 August (squares), and 17 August (diamonds). Initial severity curves are much steeper early in the epidemic than later. Solid lines are the results for the first four generations of the simulation model described in the text.

TABLE 2. Calculated ranges for the value of the ratio L_E/L_D (equation 6) for various crop, wind, and propagule parameters

Crop	Propagule particle	v_g (cm s^{-1})	LAI	H (cm)	L_D (cm)	u_* (cm s^{-1})	u_H (cm s^{-1})	L_E/L_D	Reference
Beans									
(*Phaseolus vulgaris*)	*Uromyces phaseoli*[a]	0.82–1.01	1.0–1.2	27	355–570	25–40	50–90	0.004–0.03	17,19
	U. phaseoli[a]	0.82–1.01	3.4–3.6	50	195–293	18–27	75–105	0.06–0.09	9
Winterwheat									
(*Triticum aestivum*)	Ragweed[a]	1.05	2–4	85–95	...	30–50	90–140	0.008–0.06	7
	Puccinia recondita[a]	1	2.2–3	90–100	...	29–68	75–180	0.004–0.07	3
	P. recondita[b]	1.0–1.2	0.2–2.5	10–30	250–340	...	...	0.04–0.09	26
Spring barley									
(*Hordeum vulgaris*)	*P. recondita*[b]	1.0–1.2	3.1–5.8	30–90	265–520	...	...	0.08–0.16	26
	P. recondita[b]	1.0–1.2	4.7	54	65	...	...	0.78[c]	26
Corn									
(*Zea mays*)	...	1	2.9	233	...	45–79	140–315	0.01–0.03	44

[a] Dry spores.
[b] Liquid droplets.
[c] This experiment was conducted under very low wind speeds (5 cm s^{-1} at mid-canopy).

tioned dispersive epidemic waves. Plots of logit disease severity versus $\ln(r)$ yield reasonable straight-line graphs with slopes that remain fairly constant over the course of the epidemic (Fig. 8B). The flattening of gradients late in the season may be due to the limitation in the size of the experimental plots. Similar epidemiological behavior has been reported for the spread of Septoria leaf spot in tomato (20).

The propagation velocity of the logarithmic epidemic wave depends on the relative importance of the deposition and escape of airborne spores, characterized by the ratio L_E/L_D. The calculated range of L_E/L_D for various crop and wind parameters reported in the literature are shown in Table 2. The ratio of wind speed at the top of the canopy to the friction velocity (u_H/u_*) ranges from a value of 2.2 to 4 for agricultural crops (Table 2; [3,7,9,17,19,26,44]); as a result, L_E varies between 0.5 and 1.5 H (equation 7). This result is consistent with the fact that measured vertical and downwind velocities have approximately the same magnitude within plant canopies (21,35,44). Thus, the downwind length scale for escape should be on the order of the canopy height (34,38). The settling velocities of spores are much smaller than typical wind speeds at the top of a plant canopy, and L_E/L_D tends to be much less than unity (Table 2). However, during periods of low wind speed, L_E/L_D may approach or even exceed unity (Table 2; mean wind speed measured at midcanopy = 5 cm s^{-1} [26]).

The role of intermittent wind may be very important in determining the spatio-temporal development of an epidemic (5). The effect of intermittent wind speed was investigated by running simulated epidemics with a mixed contact distribution that was a weighted sum of $CD_{MB}[a = 1/(4\ L_E)]$ and of CD given by equation 6 (with $L_E/L_D = 0.05$). In these simulations, a certain fraction, f, of the released spores was assumed to be dispersed according to CD_{MB}, and the remaining fraction, $1 - f$, was dispersed by equation 6. The dispersive nature of epidemics with $f = 1.0$, 0.9, 0.5, and 0.0 was investigated by examination of plots of isopathic velocity versus time (Fig. 9). On such a plot, isopathic velocity will approach an upper limiting value for a simple traveling wave (Fig. 9; $f = 1.0$). The resultant epidemic waves for mixed dispersal, however, are dispersive in nature, as indicated by the continued increase in the value of V as time passes (Fig. 9; $f = 0.9$ and 0.5). This is true, even if only 10% of the spores are released during turbulent conditions (Fig. 9; $f = 0.9$). An interesting result of these simulations is that epidemics generated by mixed dispersal ($f = 0.5$ and $f = 0.9$) developed more rapidly than did the epidemics resulting from either of the parental contact distributions ($f = 0.0$ and $f = 1.0$). Dispersal by equation 6 with a small value of the ratio L_E/L_D favors the spatial spread of propagules, however, overall deposition is reduced, which slows the temporal development of disease. On the other hand, a dispersal function with a finite length scale, such as CD_{MB}, limits spatial spread, while favoring the local increase in disease. The net result is that mixed dispersal favors

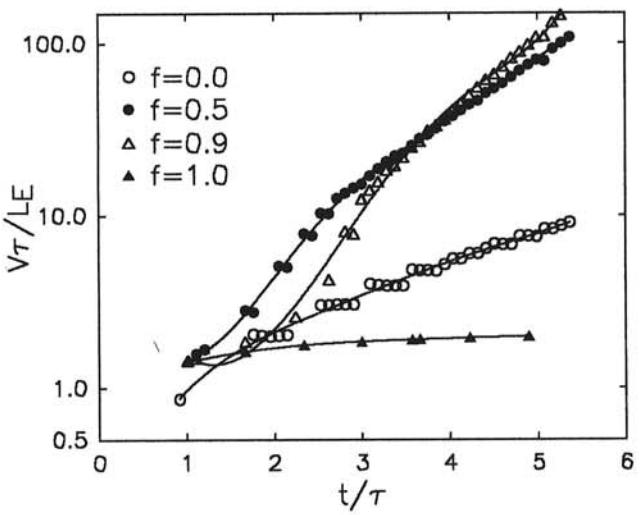

Fig. 9. The effect of a mixed contact distribution on disease development is illustrated in a plot of dimensionless isopathic velocity ($V\tau/L_E$, evaluated at the 0.5% disease severity isopath) versus dimensionless time (t/τ). It was assumed that a fraction, f, of the spores was dispersed according to CD_{MB}, and the remaining fraction ($1 - f$) was dispersed by equation 6.

very rapid disease spread and development. One generation's turbulently dispersed propagules "pioneer" new territory, and the succeeding generations' locally dispersed spores complete the process of colonization.

In summary, turbulent dispersal of propagules results in traveling epidemic waves in the log-transformed space. This type of epidemic is characterized by ever decreasing spatial gradients and continually increasing velocities of propagation. This model has the advantage of describing spatial disease gradients early in an epidemic and remains applicable until disease has spread over the entire experimental plot.

APPENDIX

Contact distribution. Assuming that wind speed and turbulence can be described by equation 5, the solution to equation 4 for a continuous ground-level point source ($z = 0$, $r = 0$) releasing spores at a rate Q_0 (Table 1) is

$$C(z,r) = Q_0\ Z(z,r)/(2\pi r\ u_H\ H) \qquad (A.1)$$

in which $Z(z,r) = B/[\Gamma(D)R^D]\ \exp\{-[(z/H)^B/R]\}$ and $B = (3 - 2b)$, $R = B^2\ K_H\ r/u_H\ H^2$, $D = (1 + B)/2B = (2 - b)/(3 - 2b)$, and $\Gamma(D)$ is the gamma function evaluated at D that is equal to $(D - 1)!$ for integral D. Equation A.1 evaluated on the ground ($z = 0$) gives a concentration that falls off as radius

to the negative $1 + D \approx 17/9 \approx 1.89$ power. This is very close to the inverse square law obtained by assuming that spores simply move away from a source in straight-line trajectories at a constant velocity (9).

Deposition. To include the effect of deposition in the above model (equation A.1), I assume that the aerial spore concentration, including deposition, can be expressed as

$$C_D(z,r) = Q(r)\, Z(z,r)/(2\pi r\, u_H\, H) \qquad (A.2)$$

in which $Z(z,r)$ is dimensionless as given in equation A.1 and $Q(r)$ (Table 1) is the rate at which airborne spores are blown through an infinitely high cylinder of radius r. This assumption is equivalent to Chamberlain's source depletion model (11). Basically, turbulent mixing is assumed to be faster than deposition, so the depletion of the spore cloud does not change the shape of its concentration profile, $Z(z,r)$. Assuming there is a uniform canopy of height, H, and leaf area index, LAI, the deposition flux per unit of ground area, $F_D(r)$ (Table 1), is given by

$$F_D(r) = -\frac{1}{2\pi r}\frac{dQ}{dr} = \frac{v_d\, Q(r)}{2\pi r\, u_H\, H^2}\int_0^H Z(z,r)dz \qquad (A.3)$$

in which v_d (Table 1) is the deposition velocity for airborne spores within the plant canopy. If deposition is by gravitational sedimentation, then $v_d = v_g\, LAI$, in which v_g (Table 1) is the gravitational settling velocity of the spores (15). Deposition to the ground may be accounted for by replacing LAI with $LAI + 1$ in the above expression for v_d. The integral in equation A.3 is evaluated by the definition of $Z(z,r)$ in equation A.1, so

$$\int_0^H Z(z,r)dz = \frac{\mathrm{B}}{\Gamma(D)R^D}\int_0^H = \exp\left[-\frac{(z/H)^B}{R}\right]dz. \qquad (A.4)$$

Making the substitutions $X = (z/H)B/R$ and $dz = [H\, R^{1/B}\, X^{1/B-1}/B]dX$, I obtain

$$\int_0^H Z(z,r)dz = \frac{H\, R^{(1-B)/2B}}{\Gamma(D)}\int_0^{1/R} X^{1/B-1}\, e^{-x}\, dX. \qquad (A.5)$$

The integral on the right side of equation A.5 is equal to $\gamma(B^{-1}, R^{-1})$, the incomplete gamma function of order B^{-1} evaluated at R^{-1} ([1], p. 260).

Using equation A.5, equation A.3 can be solved for $Q(r)$ to yield

$$Q(r) = Q_0 \exp\left[-\frac{L_E}{L_D}\int_0^R y^{\frac{(1-B)}{2B}}\frac{\gamma(B^{-1}, y^{-1})}{\Gamma(D)}\,dy\right] \qquad (A.6)$$

in which y is a dummy integration variable, L_D is the downwind length scale for deposit defined by $L_D = u_H H/v_d$, L_E is the downwind length scale for spore escape from the canopy and is defined by $L_E = r/R = u_H H^2/(B^2 K_H)$. By definition the contact distribution, $CD(r)$, is given by $F_D(r)/Q_0$, so combining equations A.3 and A.6 yields equation 6 (described in text). In the limit as $B \to 1$, equation 6 can be approximated by (15)

$$CD(r) = \frac{[r/L_E + \sqrt{1 + r^2/L_E^2}]^{-(L_E/L_D)}}{2\pi r\, L_D\sqrt{1 + r^2/L_E^2}} \qquad (A.7)$$

in which L_D and L_E are defined as above. In the limit, $L_E \to \infty$ spores remain in the canopy, and equation A.7 approaches the two-dimensional formulation suggested by McCartney and Bainbridge ([26]; i.e., $CD(r) = \exp(-r/L_D)/(2\pi r L_D)$). For $r >> L_E$, equation A.7 approaches r raised to the negative $(2 + L_E/L_D)$ power. Thus, at large distances from the foci, spore deposition falls off as a negative power of distance. The exponent in this power law becomes increasingly negative with increasing canopy leaf area or height or spore settling speed and less negative with increased turbulent mixing.

Mollison's condition. The question at hand is whether the contact distribution derived from equation 6 satisfies Mollison's condition (equation 1; [30]). I first note that the value of the incomplete gamma function is always less than the value of the corresponding gamma function, so

$$\gamma(B^{-1}, y^{-1}) < \Gamma(B^{-1}). \qquad (A.8)$$

I can obtain a lower bound by taking only the first term of a positive definite power-series expansion for the incomplete gamma function ([1], p. 262: equation 6.5.29):

$$\gamma(B^{-1}, R^{-1}) = R^{-1/B}\, e^{-1/R}\, \Gamma(B^{-1})\, \Sigma_{n=0}^{\infty}\,[R^n\, \Gamma(B^{-1} + 1 + n)]^{-1}$$

$$\gamma(B^{-1}, R^{-1}) > B\, R^{-1/B}\, e^{-1/R}. \qquad (A.9)$$

Using the upper bound for the incomplete gamma function (equation A.8) in the argument of the exponential function in equation 6 and the lower bound (equation A.9) in the premultiplier, I obtain a lower bound for the value of $CD(r)$:

$$CD(r) > \frac{R^{(1-B)/2B}\, B/R^{-1/B}\, e^{-1/R}}{2\,\pi r\, L_D\, \Gamma\,(D)}$$

$$\times \exp\left\{-(L_E/L_D)\int_0^{r/LE}\left[y^{(1-B)/2B}\frac{\Gamma\,(B^{-1})}{\Gamma(D)}\right]dy\right\}. \qquad (A.10)$$

After multiplying equation A.10 by $\exp(kR)$, recalling $R = r/L_E$ and performing the integration, I obtain

$$CD(r) > \frac{B\, L_D}{2\pi L_E\, \Gamma(D)}$$

$$\times \exp\left[k\, r - \frac{(1 + 3B)\ln(R)}{2B} - \frac{1}{R} - \frac{2L_E\Gamma\,(B^{-1})B}{L_D\,\Gamma(D)(1 + B)}R^{(1+B)/2B}\right]. \qquad (A.11)$$

Comparing the first and last terms in the argument of the exponential in equation A.11, one can see that the linear term will dominate and CD will increase indefinitely with increasing R unless $(1 + B)/(2B) > 1$. Recalling that $B = 3 - 2b$, this condition can only be true if $b > 1$, which implies unrealistically that wind speed decreases with height (equation 5). Thus, it is demonstrated that the CD given by equation 6 is not of an exponential order for realistic wind-velocity profiles.

The algorithm for the epidemic. To obtain an approximate solution to equations 10 and 11, I conceptually divide the field into subdivisions so the disease severity of the j^{th} area, A_j, at time $n \times \Delta t$ is S_j^n. This severity is the sum of latent severity, LS_j^n, which accounts for lesions not yet sporulating; infectious severity, IS_j^n, which accounts for lesions actively sporulating; and noninfectious severity, NS_j^n, which accounts for lesions no longer sporulating. The solution to equation 10 is approximated by solving the following set of finite difference equations:

$$S_j^{n+1} = SMAX - (SMAX - S_j^n)\exp(-N_j^k/SMAX \qquad (A.12)$$

$$N_j^n = M(\Delta t/i)\sum_{\text{all k}} CD(r_{jk})\, A_k\, IS_k^n \qquad (A.13)$$

$$LS_j^n = S_j^n - S_j^{[n-(i+p)/\Delta t]} \qquad (A.14)$$

$$IS_j^n = S_j^{(n-p/\Delta t)} - S_j^{[n-(i+p)/\Delta t]} \qquad (A.15)$$

$$NS_j^n = S_j^{[n-(i+p/\Delta t]}. \qquad (A.16)$$

The distance between area j and area k is $r_{jk} = [(x_j - x_k)^2 + (y_j - y_k)^2]^{1/2}$. S_j^n denotes the lesion density within area j at time $n \times \Delta t$, and N_j^n is the number of spores deposited per unit of

ground area within area j between time $n \times \Delta t$ and time $(n + 1) \times \Delta t$. Quantity $CD(r_{jk})$ is the probability density that a spore released from within the source area, A_k, is deposited within the target area, A_j, per unit of target area. $CD(r_{jk})$ was evaluated from a numerical integration of equation 6. The number of new lesions produced during each time step was calculated by accounting for multiple infection with equation A.8. Given a set of initial conditions for LS_j^0, IS_j^0, and NS_j^0, equations A.12 and A.13 can be solved iteratively at each time step to yield the total lesion density, S_j^n, within each area, j. Equations A.14–A.16 are used to apportion lesions according to sporulation characteristics at each time step.

The isopathic velocity, $V(S)$, given by equation 12, was estimated in simulations with the following finite difference algorithm:

$$V_j^n = -[(S_j^{n+1} - S_j^{n-1})/(S_{j+1}^n - S_{j-1}^n)] \times (\Delta r/\Delta t) \qquad \text{(A.17)}$$

in which Δr is the distance between the centers of contiguous areas in the direction of focus expansion and Δt is defined as above.

LITERATURE CITED

1. Abromowitz, M., and Stegun, A. S. 1964. Handbook of Mathematical Functions with Formulas, Graphs, and Mathematical Tables. Natl. Bur. Stand., Washington D. C. 1046 pp.
2. Alderman, S. C., Nutter, F. W., Jr., and Labrinos, J. L. 1989. Spatial and temporal analysis of spread of late leaf spot of peanut. Phytopathology 79:837-844.
3. Aylor, D. E. 1987. Deposition gradients of urediniospores of *Puccinia recondita* near a source. Phytopathology 77:1442-1448.
4. Aylor, D. E. 1989. Aerial spore dispersal close to a focus of disease. Agric. For. Meteorol. 47:109-122
5. Aylor, D. E. 1990. The role of intermittent wind in the dispersal of fungal pathogens. Annu. Rev. Phytopathol. 28:73-92.
6. Aylor, D. E., and Ferrandino, F. J. 1985. Escape of urediniospores of *Uromyces phaseoli* from a bean field canopy. Phytopathology 75:1232-1235.
7. Aylor, D. E., and Ferrandino, F. J., 1989. Dispersion of spores released from an elevated line source within a wheat canopy. Boundary-Layer Meteorol. 46:251-273.
8. Aylor, D. E., and Ferrandino, F. J. 1989. Temporal and spatial development of bean rust epidemics initiated from an inoculated line source. Phytopathology 79:146-151.
9. Aylor, D. E., and Ferrandino, F. J. 1990. Initial spread of bean rust close to an inoculated bean leaf. Phytopathology 80:1469-1476.
10. Berger, R. D., and Luke, H. H. 1979. Spatial and temporal spread of oat crown rust. Phytopathology 69:1199-1201.
11. Chamberlain, A. C. 1953. Aspects of travel and deposition of aerosol and vapor clouds. Rep. AERE-R 1261, Atomic Energy Res. Establish., Harwell, England.
12. Chamberlain, A. C. 1967. Transport of *Lycopodium* spores and other small particles to rough surfaces. Proc. Roy. Soc. A 290:236-265.
13. Csanady, G. T., 1973. Turbulent Diffusion in the Environment. Page 134. D. Reidel Publishing Co., Dordrecht, Netherlands. 248 pp.
14. Diekmann, O. 1978. Thresholds and traveling waves for the geographical spread of infection. J. Math. Biol. 6:109-130.
15. Ferrandino, F. J. 1989. Spatial and temporal variation of a defoliating plant disease and reduction in yield. Agric. For. Meteorol. 47:273-290.
16. Ferrandino, F. J. 1989. A distribution-free method for estimating the effect of aggregated plant damage. Phytopathology 79:1229-1232.
17. Ferrandino, F. J., and Aylor, D. E. 1984. Settling speed of clusters of spores. Phytopathology 74:969-972.
18. Ferrandino, F. J., and Aylor, D. E. 1985. An explicit equation for deposition velocity. Boundary-Layer Meteorol. 31:197-201.
19. Ferrandino, F. J., and Aylor, D. E. 1987. Relative abundances and deposition gradients of clusters of urediniospores of *Uromyces phaseoli*. Phytopathology 77:107-111.
20. Ferrandino, F. J., and Elmer, W. H. 1992. Reduction in tomato yield due to Septoria leaf spot. Plant Dis. 76:208-211.
21. Finnigan, J. J. 1979. Turbulence in waving wheat: I. Mean statistics and honami. Boundary-Layer Meteorol. 16:181-211.
22. Gregory, P. H. 1945. The dispersion of airborne spores. Trans. Br. Mycol. Soc. 28:26-72.
23. Gregory, P. H. 1968. Interpreting plant disease dispersal gradients. Annu. Rev. Phytopathol. 6:189-212.
24. Jeger, M. J. 1983. Analysing epidemics in time and space. Plant Pathol. 32:5-11.
25. McCartney, H. A., and Aylor, D. E. 1987. Relative contribution of sedimentation and impaction to deposition of particles in a crop canopy. Agric. For. Meteorol. 40:343-358.
26. McCartney, H. A., and Bainbridge, A. 1984. Deposition gradients near to a point source in a barley crop. Phytopathol. Z. 109:219-236.
27. Minogue, K. P. 1986. Disease gradients and the spread of disease. Pages 285-310 in: Plant Disease Epidemiology. K. J. Leonard and W. E. Fry, eds. Macmillan Publishing Co., Inc., New York.
28. Minogue, K. P., and Fry, W. E., 1983. Models for the spread of disease: Model description. Phytopathology 73:1168-1173.
29. Minogue, K. P., and Fry, W. E., 1983. Models for the spread of disease: Some experimental results. Phytopathology 73:1173-1176.
30. Mollison, D. 1977. Spatial contact models for ecological and epidemic spread. J. Roy. Stat. Soc. B 39:283-326.
31. Monin, A. S., and Yaglom, A. M. 1973. Statistical Fluid Mechanics: Mechanics of Turbulence. Vol. 1. Pages 657-666. The MIT Press, Cambridge, MA. 769 pp.
32. Mundt, C. C., and Leonard, K. J. 1985. A modification of Gregory's model for describing plant disease gradients. Phytopathology 75:930-935.
33. Pasquill, F. 1974. Atmospheric Diffusion. 2nd ed. Pages 349-353. Ellis Harwood, Chichester, England. 228 pp.
34. Raupach, M. R., and Thom, A. S. 1981. Turbulence in and above plant canopies. Annu. Rev. Fluid Mech. 13:97-129.
35. Shaw, R. H., Silversides, R. H., and Thurtell, G. W. 1974. Some observations of turbulence and turbulent transport within and above plant canopies. Boundary-Layer Meteorol. 5:429-449.
36. Sutton, O. G. 1932. A theory of eddy diffusion in the atmosphere. Proc. Roy. Soc. A 135:143-165.
37. Thieme, H. R. 1977. A model for the spatial spread of an epidemic. J. Math. Biol. 4:337-351.
38. Thom, A. S., 1975. Momentum, mass and heat exchange of plant communities. Pages 57-109 in: Vegetation and the Atmosphere. J. L. Monteith, ed. Vol. 1, Principles. Academic Press, Inc., New York.
39. van den Bosch, F., Frinking, H. D., Metz, J. A. J., and Zadoks, J. C. 1988. Focus expansion in plant disease: III. Two experimental examples. Phytopathology 78:919-925.
40. van den Bosch, F., Zadoks, J. C., and Metz, J. A. J. 1988. Focus expansion in plant disease: I. The constant rate of focus expansion. Phytopathology 78:54-58.
41. van den Bosch, F., Zadoks, J. C., and Metz, J. A. J. 1988. Focus expansion in plant disease: II. Realistic parameter-sparse models. Phytopathology 78:59-64.
42. Vanderplank, J. E. 1975. Plant Disease: Epidemics and Control. Academic Press, Inc., New York. 216 pp.
43. Waggoner, P. E. 1952. Distribution of potato late blight around inoculum sources. Phytopathology 42:323-328.
44. Wilson, J. D., Ward, D. P., Thurtell, G. W., and Kidd, G. E. 1982. Statistics of atmospheric turbulence within and above a corn canopy. Boundary-Layer Meteorol. 24:495-519.